RC25203 (W1108-038) August 11, 2011
Physics

IBM Research Report

Protecting Superconducting Qubits from External Sources of Loss and Heat

Antonio D. Córcoles, Jerry M. Chow, Jay M. Gambetta, Chad Rigetti, J. R. Rozen, George A. Keefe, Mary Beth Rothwell, Mark B. Ketchen, M. Steffen
IBM Research Division
Thomas J. Watson Research Center
P.O. Box 218
Yorktown Heights, NY 10598

Protecting superconducting qubits from external sources of loss and heat

Antonio D. Córcoles,[1] Jerry M. Chow,[1] Jay M. Gambetta,[1] Chad Rigetti,[1] J. R. Rozen,[1] George A. Keefe,[1] Mary Beth Rothwell,[1] Mark B. Ketchen,[1] and M. Steffen[1]
IBM T.J. Watson Research Center, Yorktown Heights, New York 10598, USA

(Dated: August 1, 2011)

We characterize a superconducting qubit before and after embedding it along with its package in an absorptive medium. We observe a drastic improvement in the effective qubit temperature and over a tenfold improvement in the relaxation time up to 5.7 μs. Our results suggest the presence of external radiation inside the cryogenic apparatus can be a limiting factor for both qubit initialization and coherence. We infer from simple calculations that relaxation is not limited by thermal photons in the sample prior to embedding, but by dissipation arising from non-equilibrium quasiparticle generation.

Energy loss in superconducting qubits remains a major object of study on the road towards scalable qubit architectures. The primary origins of relaxation in superconducting qubits can be intrinsic to the material, encompassing dielectric,[1] and resistive (quasiparticle) losses,[2,3] or external through radiative[4,5] and electromagnetic (EM) environmental losses.[6,7] The current understanding of these loss mechanisms is still incomplete, as it is difficult to experimentally separate the different contributions to qubit relaxation. It is equally critical to consider the bath to which the qubits relax, as the equilibrium temperature of such a bath determines the degree of purity for qubit initialization.[8,9] Thermal heating of qubits is well known in experiments,[10] although not often pointed out, and its elimination is necessary for future quantum computing applications.

In this Letter, we present an experiment where extrinsic loss mechanisms on a superconducting qubit are removed, resulting in both a lower effective qubit temperature and a significant increase in qubit coherence. We characterize the same superconducting qubit in two separate experimental configurations: in a printed-circuit board (PCB) package mounted within a standard cryogenic environment with no additional shielding, and then in nominally the same setup with the only change of embedding the entire PCB and qubit device in absorptive material. We find, surprisingly, that the embedding of highly sensitive quantum circuits in an absorptive, lossy medium can be useful for shielding and attenuating losses caused by radiation and EM environmental factors within the cryogenic setup.[11,12] Our experimental procedure isolates the qubit loss mechanisms to be only those which are material related or on-chip/on-package, and linked to a bath that is thermalized to near the base temperature of our setup.

The experimental device tested is a capacitively shunted flux qubit[13] (CSFQ) in the circuit quantum electrodynamics architecture. The qubit is capacitively coupled to a coplanar waveguide $\lambda/2$ resonator ($\omega_{\rm cav}/2\pi = 10.3$ GHz), with a 6 μm center strip and 3 μm spacing to ground, via a $C_{\rm qr} \sim 5$ fF interdigitated capacitor. A vacuum Rabi experiment (not shown) gives a qubit-resonator coupling strength $g/\pi \sim 200$ MHz. The resonator is also capacitively coupled to a microwave feed line ($C_{\rm c} \sim 2$ fF), with a linewidth $\kappa/2\pi = 470$ kHz, corresponding to $Q = 22,000$.

The CSFQ consists of a 15 μm-wide square loop containing three Josephson junctions, one with a smaller critical current I_0 than the other two by a ratio α, and an interdigitated shunt capacitor with 5 μm-wide fingers and gaps [Fig. 1(a-b)]. The ground plane, resonator, and feed line are patterned in Nb, whereas the Josephson junctions and the shunt capacitors are defined using Al. More fabrication details of the qubit are described in previous work[13,14].

The qubit is mounted in a custom designed multilayer copper clad FR-4 PCB, and flux biased with a hand-wound ~1000-turn coil (Cu clad Nb/Ti wire) also attached to the PCB [Fig. 1(c)]. In our first experiment, the sample package is attached to the mixing chamber of a cyrogen-free dilution refrigerator (DR) with a nominal base temperature of $\sim$ 15 mK. Figure 2 shows a schematic of the DR setup and all relevant experimental components anchored to different temperature stages.

In this configuration, spectroscopy of the qubit reveals significant steady-state thermal population. A high-power spectrum taken at a flux $\Phi = 0.51\Phi_0$ is shown in Fig. 3(a) (upper trace), in which we can identify equilibrium population in at least two excited states; we observe transitions at $\omega_{01}/2\pi = 5.3$ GHz, $\omega_{12}/2\pi = 5.58$ GHz, and $\omega_{23}/2\pi = 5.83$ GHz, where ω_{ij} is the transition frequency from state $|i\rangle$ to $|j\rangle$ in the CSFQ energy spectrum. The additional sharper peaks correspond to two-photon transitions between non-adjacent energy levels, $\omega_{02}/4\pi = 5.43$ GHz, $\omega_{13}/4\pi = 5.70$ GHz, and $\omega_{24}/4\pi = 5.89$ GHz which are seen due to the high spectroscopy power.

Time domain measurements are performed at the minimum transition frequency 5.01 GHz ("sweet spot") located at half-integer flux-quanta. We measure an energy relaxation time $T_1 = 513$ ns for this bias point, obtained from a sliding π-pulse experiment (Fig. 3(b), squares).

The spectroscopy data indicate that in the first experimenal configuration, our qubit is strongly coupled to some external energy. We performed different experiments to diagnose the source of this additional energy, first by adding and changing components in the experimental wiring in Fig. 2. Additional attenuation to all

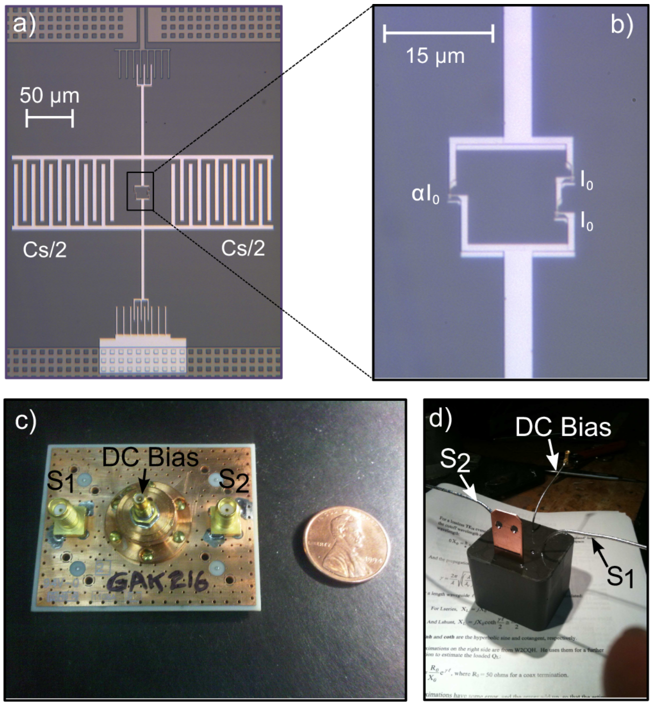

Figure 1. (a) Optical micrographs of the CSFQ device. Two ~ 5 fF interdigitated capactitors couple the CSFQ to the end of a $\lambda/2$ coplanar waveguide resonator and to ground. (b) Zoom in on qubit loop with three Al/AlOx junctions, one of them smaller than the others by $\alpha \sim 0.41$. From qubit spectroscopy, we fit to the qubit Hamiltonian and obtain the parameters $I_0 = 0.3$ μA, $\alpha = 0.41$ and $C_s = 93$ fF. (c) PCB sample package for qubit experiments. Two rf lines, S_1 and S_2, connect to an on-chip feedline to address the cavity and qubit. A ~ 1000-turn DC coil is mounted on the PCB for applying magnetic flux. (d) The device after being embedded in an absorptive epoxy. Flexible coaxial lines and a copper plate for mechanical and thermal anchoring are attached prior to the operation.

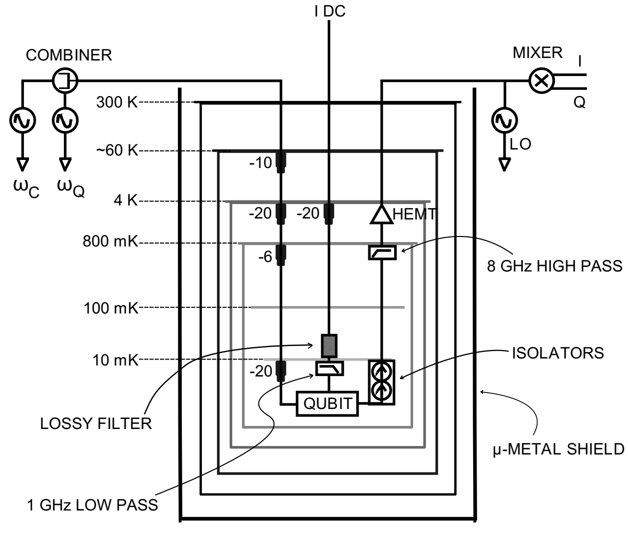

Figure 2. Schematic of experimental setup, showing relevant components on the three control lines to the qubit as well as the different temperature stages and shields.

the different stages, additional high- and low-pass filters on the input and output lines, improved heat sinking of all components, and different bandwidth isolators/circulators did not result in any noticeable qualitative improvement to heating or coherence times. However, we did observe a reduction in the effective heating on another qubit sample when it was mounted on a PCB and housed in a copper enclosure. Although that qubit still showed some signature of heating, that phenomenological result combined with recent work from the UCSB group[15] suggesting increased resonator losses due to infrared radiation motivated us to completely eliminate the effect of external radiative and environmental energy sources.

To protect the previously measured qubit and its sample package from external radiation, we place it in a mold and submerge it with CR-124 ECCOSORB epoxy (Emerson & Cuming). The resin is cured at 70°C for over 12 hours. Flexible coaxial lines are used to provide connections to the input and output of the feedline as well as to the DC coil and a copper post is added for mechanical support and thermal anchoring [Fig. 1(d)] prior to embedding.

Without changing any components interior to the cryostat setup shown in Fig. 2, we recharacterize the sample and find substantial improvements to the qubit properties. In fig. 3(a), the qubit spectroscopy at the same $\Phi = 0.51\Phi_0$ flux bias shows remarkably fewer peaks. In the new experiment, only the transition corresponding to the $|0\rangle \to |1\rangle$ transition at $\omega_{01}/2\pi = 5.3$ GHz is visible. The spectroscopy power is kept constant in both situations, and in this case is still strong enough to permit the two-photon $|0\rangle \to |2\rangle$ transition at $\omega_{02}/4 = 5.43$ GHz.

The qubit relaxation and coherence times also improve dramatically as a result of the embedding. $T_1^{\rm b}$ (we use the superscript 'b' to denote the results post embedding) of the qubit biased to the flux sweet spot increases by a factor of 10, from 513 ns previously to 5.7 μs [Fig. 3(b)]. A Ramsey fringe experiment is performed giving a decoherence time $T_2^{*,\rm b} = 5.6\mu$s. However, by performing a spin echo measurement with a refocusing π-pulse in between two $\pi/2$-pulses, we extract $T_2^{\rm b} = 9.4$ μs, nearly twice $T_1^{\rm b}$ (Fig. 3(b) inset). The measurement that $T_2^{\rm b} \neq T_2^{*,\rm b}$ is most likely due to residual $1/f$ flux noise[16]. From the measurements of $T_1^{\rm b}$ and $T_2^{*,\rm b}$ we estimate a pure dephasing time $T_\phi^{\rm b} \sim 11$ μs, which is comparable with recent experiments of highly-coherent Josephson junction qubits.[17]

Whereas 5.7 μs was the highest $T_1^{\rm b}$ value measured, repeated measurements over a period of a week yielded values for $T_1^{\rm b}$ between ~ 3.5 and ~ 5.7 μs. We hypothesize that this variation in relaxation times could be due to slow fluctuations in dielectric loss. Future experiments will address this possibility.

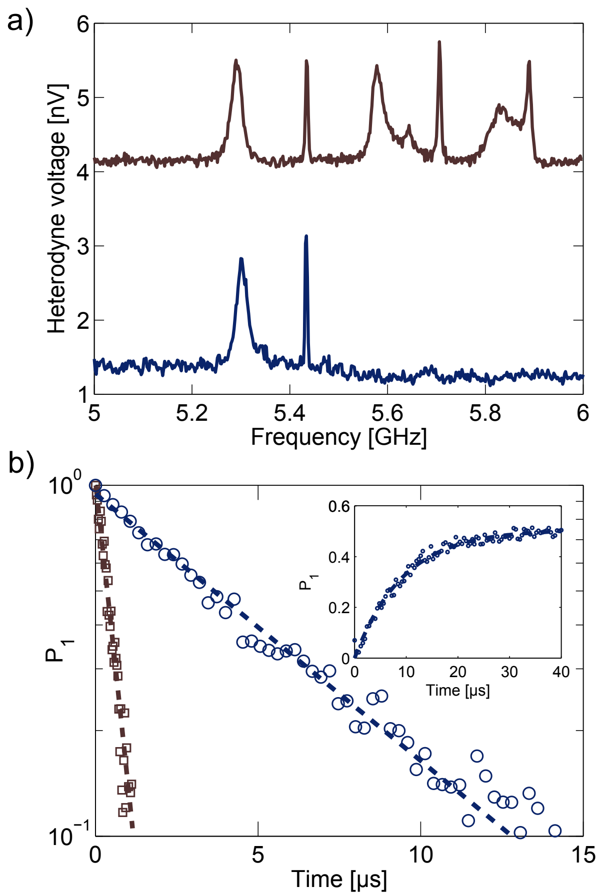

Figure 3. (a) Qubit spectroscopy at $0.51\Phi_0$ before (upper trace) and after (lower trace) embedding the sample in eccosorb. The three narrow peaks at 5.43, 5.70 and 5.89 GHz in the upper trace correspond to the multi-photon transitions $|0\rangle \to |2\rangle$, $|1\rangle \to |3\rangle$ and $|2\rangle \to |4\rangle$, respectively. The broader peaks are the qubit bare transitions. The population of excited states in the qubit, arising from thermal excitations, is absent in the lower trace. (b) Energy relaxation time T_1 before (squares) and after (circles) applying the eccosorb. T_1 increased by a factor of 10. An echo measurement of T_2 on the potted sample (inset) gave $T_2 = 9.4\mu$s, very close to $2T_1$.

The dramatic improvement in the qubit relaxation rate and the reduction of the effective qubit temperature give us clues about the mechanism and source of the external losses. Inside the DR, although the sample is firmly linked to the $\sim$ 15 mK mixing chamber plate, the still shield surrounds the entire sample space, providing a source of 800 mK blackbody radiation to impinge upon the sample package.

We consider physical processes by which radiation inside the DR can result in a thermally excited equilibrium qubit state. First, there is the mechanism of direct qubit excitation at 5 GHz due to blackbody radiation. Using a Planck's law calculation, the mean thermal photon number at 5 GHz due to an 800 mK radiator is estimated to be ~ 3. However, given the large volume of the DR, the small solid angle around the sample package, and attenuation by the sample package the probability of these few photons reaching the qubit are likely very small. Furthermore, to match our tenfold coherence time improvement, we estimate the effective temperature of a 50 Ω bath to which the qubit relaxes[6] to be $\sim$ 1.3 K, using the expression $T_1^{\rm b} = T_1 \coth(\hbar\omega/2k_{\rm B}T)$. This value is not consistent with the inferred temperature from spectroscopy [Fig. 4(a-b)] and the higher equilibirum temperature is unlikely to be due to any direct qubit transitions caused by radiative sources in the DR.

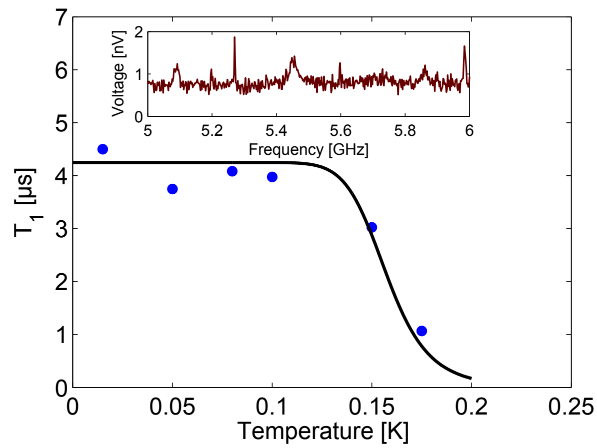

Figure 4. T_1 versus mixing chamber temperature. The drop off of T_1 above 150 mK is in agreement with quasiparticle generation (theory solid line). Spectroscopy (inset) and T_1 at 175 mK are in good qualitative agreement with the first experiment prior to the embedding process.

Another external loss process we consider is the generation of non-equilibrium quasiparticles due to the radiation of energy (> 80 GHz) which exceeds the superconducting gap of Al ($\Delta \sim 200\ \mu$eV). The non-equilibrium quasiparticles have a detrimental effect on the performance of the qubit through dissipation[3] and tunneling across the junctions.[2]

To mimic the effect of non-equilibrium quasiparticles on the first experiment, we repeat spectroscopy and relaxation time measurements on the embedded sample at higher mixing chamber temperatures. Figure 4 shows T_1 versus sample temperature, with a roll-off around 160 mK. This behavior with increased temperature is qualitatively in agreement with recent theory of qubit relaxation due to non-equilibrium quasiparticles.[2] At 175 mK, we find $T_1 \sim 700$ ns and a spectrum which shows up to 3 transitions (Fig. 4 inset), reminiscent of the original experiment. Therefore, prior to the embedding procedure, we nominally attribute both the degraded coherence and the heating of the qubit to quasiparticles generated by radiation within the DR.

Although the embedded qubit has a quality factor of $\sim 1.8 \times 10^5$, this is still substantially below the limit placed by spontaneous decay through the resonator.[7,18] Candidates for the origin of the actual limit include spurious coupling to unwanted EM modes in the package[19] and dielectric losses arising from native oxides on the Al defining the qubit shunt capacitors.[13,17,20] Future experiments will address these issues in greater detail.

To conclude, we have demonstrated that environmental radiation can have severe detrimental effects on a superconducting qubit, both in terms of coherence and effective temperature, most likely due to the generation of nonequilibrium quasiparticles. With the simple procedure of embedding the sample package in a lossy epoxy material, the same qubit has remarkably improved parameters. This result is a major step for improving coherence and paves the way for determining intrinsic loss mechanisms in superconducting qubits.

We acknowledge engaging discussions with Blake Johnson and Chris Lirakis. The views expressed are those of the author and do not reflect the official policy or position of the Department of Defense or the U.S. Government.

REFERENCES

[1] J. M. Martinis, K. B. Cooper, R. McDermott, M. Steffen, M. Ansmann, K. D. Osborn, K. Cicak, S. Oh, D. P. Pappas, R. W. Simmonds, and C. C. Yu, Phys. Rev. Lett. **95**, 210503 (2005).

[2] G. Catelani, J. Koch, L. Frunzio, R. J. Schoelkopf, M. H. Devoret, and L. I. Glazman, Phys. Rev. Lett. **106**, 077002 (2011).

[3] M. Lenander, H. Wang, R. C. Bialczak, E. Lucero, M. Mariantoni, M. Neeley, A. D. O'Connell, D. Sank, M. Weides, J. Wenner, T. Yamamoto, Y. Yin, J. Zhao, A. N. Cleland, and J. M. Martinis, arXiv:1101.0862 (2011).

[4] J. M. Sage, V. Bolkhovsky, W. D. Oliver, B. Turek, and P. B. Welander, J. Appl. Phys. **109**, 063915 (2011).

[5] J. Wenner, R. Bialczak, M. Lenander, E. Lucero, M. Mariantoni, M. Neeley, A. O'Connell, D. Sank, H. Wang, M. Weides, T. Yamamoto, Y. Yin, A. Cleland, and J. Martinis, APS Meeting Abstracts , 26009 (2010).

[6] R. J. Schoelkopf, A. A. Clerk, S. M. Girvin, K. W. Lehnert, and M. H. Devoret, "Qubits as spectrometers of quantum noise," (2002).

[7] A. A. Houck, J. A. Schreier, B. R. Johnson, J. M. Chow, J. Koch, J. M. Gambetta, D. I. Schuster, L. Frunzio, M. H. Devoret, S. M. Girvin, and R. J. Schoelkopf, Phys. Rev. Lett. **101**, 080502 (2008).

[8] D. Walls and G. Milburn, *Quantum Optics*, 1st ed. (Springer, 1995) p. 351.

[9] M. A. Nielsen and I. L. Chuang, *Quantum Computation and Quantum Information* (Cambridge University Press, Cambridge, 2000).

[10] M. H. Devoret and R. J. Schoelkopf, (2011), private communications.

[11] R. Barends, J. Wenner, M. Lenander, Y. Chen, R. C. Bialczak, J. Kelly, E. Lucero, P. O'Malley, M. Mariantoni, D. Sank, H. Wang, T. C. White, Y. Yin, J. Zhao, A. N. Cleland, J. M. Martinis, and J. J. A. Baselmans, arXiv:1105.4642 , (2011).

[12] The manuscript by Barends et al. (2011) was released during the composition of this manuscript.

[13] M. Steffen, S. Kumar, D. P. DiVincenzo, J. R. Rozen, G. A. Keefe, M. B. Rothwell, and M. B. Ketchen, Phys. Rev. Lett. **105**, 100502 (2010).

[14] M. Steffen, F. Brito, D. DiVincenzo, M. Farinelli, G. Keefe, M. Ketchen, S. Kumar, F. Milliken, M. B. Rothwell, J. Rozen, and R. H. Koch, Journal of Physics: Condensed Matter **22**, 053201 (2010).

[15] R. Barends, N. Vercruyssen, A. Endo, P. de Visser, T. Zijlstra, T. M. Klapwijk, P. Diener, S. J. C. Yates, J. J. A. Baselmans, H. Wang, M. Hofheinz, J. Wenner, M. Ansmann, R. C. Bialczak, M. Lenander, E. Lucero, M. Neeley, A. D. O'Connell, D. Sank, M. Weides, A. N. Cleland, and J. M. Martinis, in *CSQ Program Review Poster* (San Diego, CA, 2011).

[16] F. Yoshihara, K. Harrabi, A. O. Niskanen, Y. Nakamura, and J. S. Tsai, Phys. Rev. Lett. **97**, 167001 (2006).

[17] H. Paik, D. I. Schuster, L. S. Bishop, G. Kirchmair, G. Catelani, A. P. Sears, B. R. Johnson, M. J. Reagor, L. Frunzio, L. Glazman, and R. J. Schoelkopf, arXiv:1105.4652 (2011).

[18] E. M. Purcell, Phys. Rev. **69**, 681 (1946).

[19] J. Wenner, M. Neeley, R. C. Bialczak, M. Lenander, E. Lucero, A. D. OConnell, D. Sank, H. Wang, M. Weides, A. N. Cleland, and J. M. Martinis, Supercond. Sci. Technol. **24**, 065001 (2011).

[20] A. D. Corcoles, J. M. Gambetta, J. M. Chow, C. Rigetti, J. Rozen, G. Keefe, M. B. Rothwell, M. Ketchen, and M. Steffen, "Energy relaxation mechanisms in capacitively shunted flux qubits," (2011), in preparation.